Shamil H. Hussein[1], Prof. Dr. Khalid K. Mohammed[2]

University of Mosul, College of Engineering, Mosul, Iraq
ORCID: orcid.org/0000-0003-1562-5372;

doi:10.15199/48.2023.05.26

Physical Modelling of the Quantum Well Asymmetric Spacer Tunnel Layer Diodes for High Frequency Applications

Abstract. *A complete description of physical models of the novel Quantum Well Asymmetric Spacer Tunnel Layer Diodes (QW-ASPATs) is simulated and compared to the standard GaAs/AlAs and InGaAs/AlAs ASPAT diodes in this work. The design and analysis of the both standard and new QW-ASPAT diodes have been investigated using numerical modeling in SILVACO ATLAS software. The impact of different structures design on crucial parameters, the junction resistance (R_j), curvature coefficient (K_v), junction capacitance (C_j), and series resistance (R_s) at zero bias detection were evaluated using a created SILVACO model. The effects of changing the AlAs barrier and quantum well layer thicknesses were carefully studied. The mesa size area of the ASPAT devices was taken into consideration and its effects to the DC and RF characteristics at zero bias voltage supply. The introduction of the well layer for the $In_xGa_{1-x}As$ structure to the barrier layer, allowed an increase in the (K_v) while maintaining a low of the (R_j). So, the QW-ASPAT devices were proposed and compared with the standard ASPAT diodes. It was found that the extracted (K_v) is increased from $13V^{-1}$ to $32.5V^{-1}$ for GaAs structure and from $12.6V^{-1}$ to $33V^{-1}$ for $In_{0.53}Ga_{0.47}As$ ASPAT at zero bias. Also, the cut off frequencies of a mesa size 4×4 μm^2 QW-ASPATs is reported about 143GHz and 303GHz for both proposed QW-ASPAT structures respectively. This work is presented to assist researchers working on ASPAT devices, including helpful predictions for optimum design parameters in order to maximize the performance of microwave devices used in the implantable medical applications.*

Streszczenie. *W niniejszej pracy przeprowadzono symulację pełnego opisu modeli fizycznych nowatorskich diod kwantowo-dołkowo-asymetrycznych z przekładką tunelową (QW-ASPAT) i porównano je z konwencjonalnymi diodami GaAs/AlAs i InGaAs/AlAs ASPAT. W niniejszej pracy zbadano konstrukcję i analizę diod ASPAT wykorzystaniem modelowania numerycznego w programie SILVACO ATLAS. Za pomocą stworzonego modelu SILVACO oceniono wpływ różnych projektów konstrukcji na cztery kluczowe parametry: rezystancję złącza (R_j), współczynnik krzywizny (K_v), pojemność złącza (C_j) i rezystancję szeregową (R_s) przy detekcji zerowej polaryzacji. Skutki zmiany bariery AlAs i grubości warstw studni kwantowej zostały dokładnie zbadane. Uwzględniono wielkość obszaru mesy urządzeń ASPAT i jej wpływ na charakterystyki DC i RF przy zerowym napięciu zasilania. Wprowadzenie warstwy zagłębienia dla struktury InGaAs do warstwy barierowej umożliwiło wzrost K_v przy jednoczesnym utrzymaniu niskiego (R_j). Zaproponowano więc urządzenia QW-ASPAT i porównano je ze standardowymi diodami ASPAT. Stwierdzono, że wyekstrahowany (K_v) wzrasta z $13V^{-1}$ do $32,5V^{-1}$ dla struktury GaAs oraz z $12,6V^{-1}$ do $33V^{-1}$ dla $In_{0,53}Ga_{0,47}As$ ASPAT przy zerowej polaryzacji. Również częstotliwości odcięcia QW-ASPAT o rozmiarze mesy 4x4 μm^2 są zgłaszane odpowiednio na około 143GHz 303GHz dla obu struktur. Niniejsza praca ma pomóc naukowcom pracującym nad urządzeniami ASPAT, w tym pomocne prognozy dotyczące optymalnych parametrów projektowych w celu maksymalizacji wydajności urządzeń mikrofalowych stosowanych w implantowanych zastosowaniach medycznych.* (***Fizyczne modelowanie diod z asymetryczną warstwą tunelu dystansowego studni kwantowej dp zastosowań o wysokiej częstotliwości***)

Keywords: Quantum tunnelling, ASPAT didoes, SILVACO atlas, and High frequency detectors.
Słowa kluczowe: Tunelowanie kwantowe, diody ASPAT, atlas SILVACO i detektory wysokiej częstotliwości.

Introduction

Wireless networks with high data rate and high speed communication have grown significantly in recent years [1]. One of the important electrical devices, tunnel diodes, can meet the requirements of low-power, high-speed mixed-signal wireless integrated circuits[2][3]. Tunneling is a quantum mechanical phenomenon that allow lower energy carriers to pass through a higher energy barrier[4]. The tunnelling diode based on GaAs platform has been proposed for high frequency applications and operation as a zero-bias detectors [5][6]. One of the important types of tunnel diodes is the asymmetric spacer tunnel layer diodes (ASPATs)[7][8]. The first attempt to explain the ASPAT diode was suggested by Syme et al. [9]. This diode consists of a thin-AlAs barrier layer [Ten monolayers(MLs)] arranged in around two undoped spacers (1,2) and asymmetrical-layer thickness with a 40:1 ratio. Due to the asymmetrical arrangement of the epitaxial spacers layer, these devices have asymmetrical I-V characteristics [10]. While ASPAT exhibit some preferred features over currently nearby universal Schottky diodes, such as insensitivity of the temperature and high resistance to pulse fatigue [11]. In the same time, the figure of merit for any detectors diode is the curvature coefficient (K_v) which different from design to other and it's represent the second derivative divided to the first derivative of the current-voltage(I-V) curve as shown in Eq. (1) below. The key K_v of the Schottky-barrier-diode(SBD) is arrived to $40V^{-1}$, while the (Sb) based tunnel diode with K_v of $47V^{-1}$ and the Germanium(Ge) based diodes are $70V^{-1}$[12][13]. The highest number reported of K_v for ASPAT diodes are $11V^{-1}$ and $32V^{-1}$ for Standard and Quantum-Well GaAs devices, respectively[14]. Furthermore, there are several parameters of the physical design that are affected on the characteristics such as junction resistance (R_j), series resistance (R_s), and Junction capacitance(C_j).

In 2021 [15], the authors proposed a two new diodes with a barrier-well heterostructure for microwave application. One is based on the GaAs scheme and the other is based on the $In_xGa_{1-x}As$ network identical to Indium phosphide (InP). But, the K_v parameters obtained are little about $10.5V^{-1}$ and $11V^{-1}$ for GaAs and InGaAs diodes repectively. In the same year, Salhi, Hadfield, and et. investigated the design of ASPAT-diode using numerical analysis in the SILVACO Atlas software [16]. They studied and evaluated different standard design of ASPAT and its effected on the junction resistance and curvature coefficient at zero bias voltage. It is observed that they obtained of the K_v value is about $13V^{-1}$ and R_s of 23Ω.

In this work, we proposed a new two structures of the ASPATs devices in order to increase the K_v compared with conventional ASPAT tunnel diode. The proposed QW-ASPAT diodes (QW-GaAs and QW-InGaAs) are modelled physically by using SILVACO simulation. The model has taken into account a number of structural parameters, the spacers layer width, and the thickness of the AlAs barrier and quantum well. It also emphasizes the significance of incorporating an QW-$In_xGa_{1-x}As$ opposite to the barrier thick to lower R_j and increase K_v. It was found that the extracted K_v is increased from $13V^{-1}$ to $32.5V^{-1}$ for GaAs structure and from $12.6V^{-1}$ to $33V^{-1}$ for $In_{0.53}Ga_{0.47}As$ ASPAT at zero bias. Also, the cut_off frequencies of a mesa size 4×4 μm^2 QW-ASPATs is reported about 143GHz and 303GHz for both structures respectively.

(1) $$K_v = \frac{\partial^2 I}{\partial^2 V} / \frac{\partial I}{\partial V}$$

Physical models of the ASPAT devices

In this paper, the ASPATs diode structure was mounted on GaAs platforms. SILVACO ATLAS software is used to design and analysis of the different ASPAT devices such as standard diodes and QW-ASPAT structures based on $In_{0.18}Ga_{0.82}As$ and $In_{0.8}Ga_{0.2}As$ for both above standard respectively. The reference ASPATs structure (GaAs and InGaAs) and new devices QW-ASPATs have the epitaxial-layer model are reported in table 1, and table 2 respectively. A single Thin-AlAs barrier is placed in a GaAs and InGaAs crystal with asymmetric spacer layers in the active epitaxial-layers. Also, a single thin well un-doped layer is placed in the both new device QW ASPAT structure (QW-GaAs and QW-InGaAs). On either side of the active layers, heavily doped contact layers and light emitting and collecting layers are developed [17]. To achieve (Γ_Γ) direct-tunnel as next to the typical indirect-AlAs band-gap carrier transport, the barrier thick was kept at 10 MLs (2.83nm).

The current-voltage (I-V) ASPAT characteristics were simulated using the semiconductor-insulator-semiconductor (SIS)model. In order to determine the probability of the electon transmission as a related to energy T(E), the SIS model solves the schrodinger-equation using the transfer matrix approach. Then, the current density of the devices is evaluated by Eq. (2). The variable parameters are the Material-effective-mass (m*), (k) is boltzmann constant, and (h) is the planck-constant. The fermi-levels (F_L) of the spacer layers sandwiched between two sides (Right and Left) of the barrier are E_{Fr} and E_{Fl}.

(2) $$J = \frac{qm^* kT}{2\pi^2 h^3} \int_0^\infty T(E) \ln\left\{ \frac{1 + e^{\frac{E_{Fr} - E}{kT}}}{1 + e^{\frac{E_{Fl} - E}{kT}}} \right\} dE$$

SILVACO ATLAS Software was used to simulate models of the all ASPAT diodes in this work. 7-regions were specified for the devices, each of which corresponded to an epitaxial layer. The mesh model of the QW-ASPAT is illustrated in Fig. 1. The biasing condition is necessary for collector and emitter regions. The central-regions with the Barrier structures were regarded as Non-equilibrium by using the S-I-S solver, whereas the left and right region of the emitter, and collector contacts are equilibrium. Biased devices allow the band structure to bend, which enables an accumulation-layer to form at the barrier's base.

Table 1. Epitaxial layer structures of the both standard ASPATs devices

Thick [nm]	GaAs/AlAs		$In_{0.53}Ga_{0.47}As$/AlAs	
	Layers	doping [cm^{-3}]	Layers	Doping [cm^{-3}]
300	GaAs Ohmic-1	$4x10^{18}$	$In_{0.53}Ga_{0.47}As$ (Ohmic-1)	$1.5x10^{19}$
35	GaAs Emitter	$1x10^{17}$	$In_{0.53}Ga_{0.47}As$ (Emitter)	$1x10^{17}$
5	GaAs spacer-1	.....	$In_{0.53}Ga_{0.47}As$ (spacer-1)	.....
2.83	AlAs Barrier	.....	AlAs (Barrier)	.....
200	GaAs spacer-2	.....	$In_{0.53}Ga_{0.47}As$ (spacer-2)	.....
35	GaAs Collector	$1x10^{17}$	$In_{0.53}Ga_{0.47}As$ (Collector)	$1x10^{17}$
350	GaAs Ohmic-2	$4x10^{18}$	$In_{0.53}Ga_{0.47}As$ (Ohmic-2)	$1.5x10^{19}$

Table 2. Epitaxial layer structures of the both proposed QW-ASPAT devices

Thick [nm]	QW- GaAs		QW- $In_{0.53}Ga_{0.47}As$	
	Layers	Doping [cm^{-3}]	Layers	Doping [cm^{-3}]
300	GaAs Ohmic-1	$4x10^{18}$	$In_{0.53}Ga_{0.47}As$ (Ohmic-1)	$1.5x10^{19}$
35	GaAs Emitter	$1x10^{17}$	$In_{0.53}Ga_{0.47}As$ (emitter)	$1x10^{17}$
5	GaAs spacer-1 $In_{0.18}Ga_{0.82}As$	-----	$In_{0.53}Ga_{0.47}As$ (spacer-1) $In_{0.8}Ga_{0.2}As$	-----
6	Well	-----	Well	-----
2.83	AlAs Barrier	-----	AlAs (Barrier)	-----
200	GaAs spacer-2	-----	$In_{0.53}Ga_{0.47}As$ (spacer-2)	-----
35	GaAs Collector	$1x10^{17}$	$In_{0.53}Ga_{0.47}As$ (Collector)	$1x10^{17}$
350	GaAs Ohmic-2	$4x10^{18}$	$In_{0.53}Ga_{0.47}As$ (Ohmic-2)	$1.5x10^{19}$

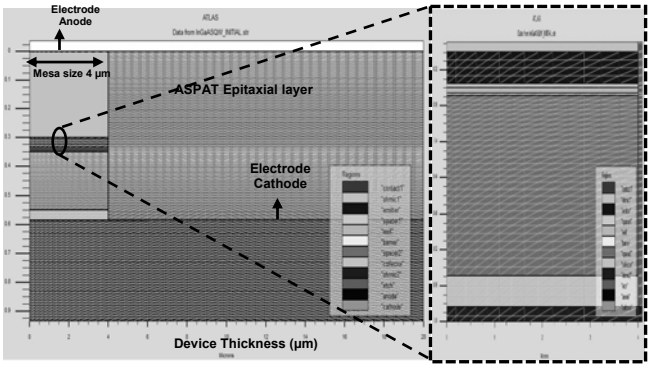

Fig.1. Mesh structure of the both new proposed QW-ASPAT diode

Fig. 2(a) displays the conduction band characteristics of a typical GaAs ASPAT at forward, zero, and reverse bias. When the bias is in the forward direction, electrons build up at the AlAs barrier's base and tunnel through it. There is a significantly decreased current flow when the bias is reversed because the band does not bend sufficiently to permit the formation of this accumulation layer. Fig. 2(b) explained the conduction bands for all ASPAT structures. In the zero bias, a significant variation in the currents flow between reverse, and forward biases are required to increase K_v. The quantum-well is added to the thin-spacers sides of the diodes. As a result, the AlAs-barrier 's height in the reverse bias is greater than forward bias. Fig. 3(a), illustrates the Conduction Band(C-B)models for both QW ASPATs diodes with a 6 nm well thickness. Fig. 3(b) shows the C-B profile of all these devices around the AlAs barrier at normal tempreture of 300°K.

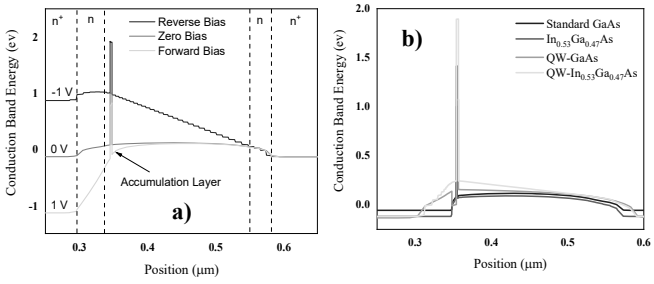

Fig. 2. a) Conduction-band profiles under different bias. b) Conduction-band profile for all ASPAT devices at zero bias.

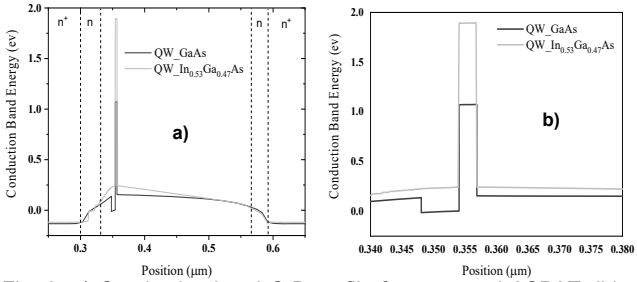

Fig. 3. a) Conduction-band C-B profile for proposed ASPAT didoe at zero bias. b) C-B band for devices in a) with 6nm well thickness.

Simulation results and discussion

DC Characteristics of ASPAT physical models

The DC characteristics of the standard ASPATs diode and new proposed QW ASPAT were simulated for a size device of 4×4μm² using SILVACO atlas. With bias step of 0.01 V at 300°k, the I-V characteristic was simulated in the range of -2V to 2V. From the IV simulated data, the important parameters (R_j) and (K_v) were extracted. The DC-simulated data of the reference GaAs-ASPAT diode at all mesa size areas such as 4×4μm², 6×6μm², and 10×10μm² as shown in Fig. 4 (a). It's observed that the current flow through diodes is reduced when the mesa size device is increased. Therefore, in this paper we take a 4×4 μm² size device. Fig. 4(b) displays the IV characteristics for all ASPAT devices on logarithmic scale. As can be seen from this figure, The QW ASPAT diode has a very small leakage-current when compared with GaAs ASPAT. The currents flow of the QW GaAs and QW InGaAs are about 9.5μA and 0.88μA at -2V bias respectively. While the currents for the GaAs and InGaAs at same mesa size device are 72μA and 62μA respectively. The key parameter value K_v for both proposed new structures (QW_GaAs and QW_InGaAs) improved and increased at zero bias voltage to $32.5V^{-1}$ and $33V^{-1}$ compared with $13V^{-1}$ and $12.6V^{-1}$ for both standard devices respectively as shown in Fig. 4(c). However, as can be shown in Fig. 4 (d), the addition of the quantum-well to barrier layer has increased R_j.

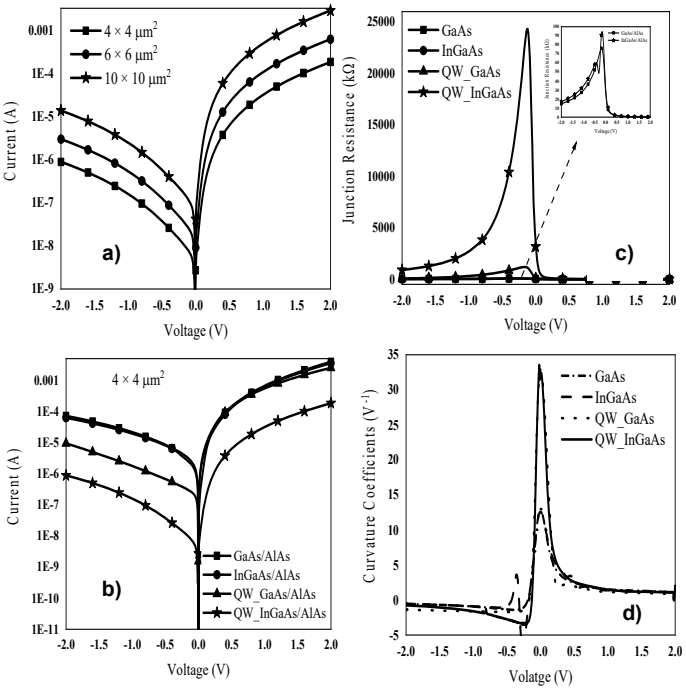

Fig. 4. a) The simulated I-V characteristic of GaAs-ASPAT diode al size device. b) The IV characteristic of ASPAT diodes at mesa area of 4×4μm². c) The junction resistances R_j extracted for all devices at size area of 16μm². d) Extracted curvature coefficient K_v of the standard and quantum well ASPAT diodes.

RF Characteristics of ASPAT physical models

The scattering parameters (S_{11}) of the proposed ASPAT diodes were obtained by using RF-Characteristic at a range of frequencies (40MHz-40GHz) with 40MHz step size. The key parameters of the RF propoerties are (C_j) and (R_s) were extracted using an equivalent circuit which built in advanced design system ADS software. The data simulated of the all devices were created at 300°k, and voltage from -0.6V to 0.6V. Fig. 5 (a) shows the variation in the C_j of the both standard and new QW diodes for a mesa size of 16μm². Fig. 5 (b) describes the R_s value of the ASPAT diodes. Despite having comparable fully depleted capacitances at about -0.6V, the devices had larger C_j at forward bias. The accumulating region at the device barrier's base is increases capacitance when it is biased forward.

In the same manner, The R_s of the ASPAT devices increase under zero and forward bias voltage, matching the behavior of calculated C_j. This is because the layer of undoped spacers is not completely depleted. Compared to the standard ASPAT, the new QW-ASPAT devices consistently show lower Rs. This is because the QW ASPATs have higher doping of the ohmic contact layer about $1.5x10^{19}cm^{-3}$ compared with $4x10^{18}cm^{-3}$ for GaAs. Thus, which results in enhanced electron mobility.

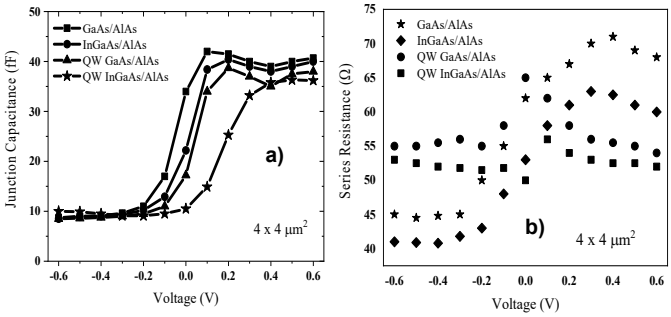

Fig. 5. a) Extracted C_j of 4×4 μm² ASPAT diodes plotted as a function of bias voltage. b) R_s of 4×4μm² for the same devices in a).

The another key parameter that evaluate ASPAT devices are the cut off frequency (f_c) and operating frequency (f_o). The (f_o) frequency represent a 1/3 value of the f_c. The evaluation of the f_c value depended on the R_s and C_j extracted from the RF properties for these devices. The f_c can be determined by Eq. (3). Table 3 shows the complete key parameters extracted at zero bias for the mesa size of 16μm² ASPAT devices. This table shows that the QW-GaAs and QW-InGaAs devices have higher f_c frequencies than the GaAs and InGaAs devices.

$$f_c = \frac{1}{2\pi R_s C_j} \tag{3}$$

Table 3. Parameters extracted at zero bias for 4×4μm² ASPATs

ASPAT Devices Structure	K_v [V^{-1}]	R_j [kΩ]	R_s [Ω]	C_j [fF]	f_c [GHz]	f_o [GHz]
Standard GaAs/AlAs	13	24	62	34	75	25
Standard $In_{0.53}Ga_{0.47}As$/AlAs	12.6	30.5	53	22.2	135	45
QW-GaAs/AlAs based on 6nm well $In_{0.18}Ga_{0.82}As$	32.5	126	65	17.2	143	47
QW-InGaAs/AlAs based on 6nm well $In_{0.8}Ga_{0.2}As$	33	3170	50	10.5	303	101

Effect of barrier (t_b) and well thickness (t_w)

In this section, we described the effect of the thick AlAs-Barrier (t_b) for DC-characteristic of the standards and quantum-well ASPAT devices at zero bias detection and

mesa size of 16μm^2. The I-V Characteristic of the proposed QW ASPAT diodes for various thickness of t_b are shown in Fig. 6. When the (t_b) is decreased from (14 to 4)MLs, the I-V Characteristic show Asymmetric-behavior, forward and reverse current rise by two orders of magnitude. This is to be expected as the thickness of the barrier has an exponentially impact on the electron tunneling through it.

Fig. 6. change of the I-V characteristic at zero bias as a function of the Barrier of diodes. (a) QW-InGaAs with thick-well of 6nm, and (b) QW-GaAs with 6nm well ASPAT device. Table 4 lists the comparable R_j and K_v values at zero bias. Reducing the tb barrier from (10 to 4) MLs reduces the value of K_v, also, it decreases that value of R_j from 24kΩ to 50Ω for the standard GaAs ASPAT diodes. R_j is decreased to less than 50Ω at the expense of K_v by further reducing the thickness of AlAs barrier to less than 4MLs. In view of this, using a thin barrier is desirable for real didoe applications, at least in terms of low R_j. But, the design of the high frequency ASPAT structures need to be further enhanced in order to achieve the selected K_v >20V^{-1} and the R_j is low. Therefore, the new structure has been proposed to improve the value of K_v. It is observed from table 4, K_v was increased to 32.5V^{-1} and 33V^{-1} for both proposed structures QW GaAs and QW InGaAs.

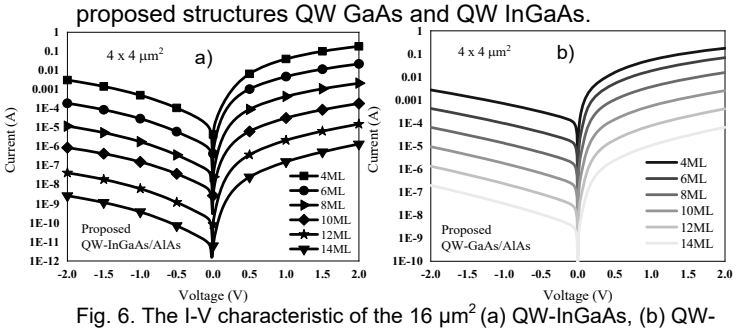

Fig. 6. The I-V characteristic of the 16 μm^2 (a) QW-InGaAs, (b) QW-GaAs when changed thick t_b at zero bias operation.

Table 4. Effect of the barrier-thick for 16μm^2 ASPAT at zero bias detection

ASPAT devices	Standard GaAs/AlAs		Standard InGaAs/AlAs		Proposed QW GaAs/AlAs		Proposed QW InGaAs/AlAs	
barrier Thick	K_v [V^{-1}]	R_j [kΩ]	K_v [V^{-1}]	R_j [kΩ]	K_v [V^{-1}]	R_j [kΩ]	K_v [V^{-1}]	R_j [kΩ]
4ML	10.6	0.05	11.5	0.001	28.5	0.25	28.6	2.34
6ML	12.3	0.4	12.4	0.31	29	1.88	29.8	20.6
8ML	12.4	2.9	12.5	3	29.5	15	32.3	33
10ML	12.6	24	13	30.5	32.5	126	33	3170
12ML	12.6	197	13.2	307	32.2	1000	32.8	0.1 G
14ML	13.4	1560	13.5	3000	32	8500	32.5	1.6 G

Conclusions

SILVACO ATLAS software has been used to model ASPAT diodes numerically and physically. Firstly, the standard ASPAT diodes and quantum-well ASPAT devices (QW-GaAs and QW-InGaAs) has been designed, analysis, and comparison performances and characteristics with each other as shown in table 4. Of note, novel well-barrier QW_ASPAT diodes proposed to enhance the Curvature coefficient (K_v), Junction resistance (R_j), Junction capacitance (C_j), and Series resistance (R_s). The simulated results show that the K_v is improved from 13V^{-1} to 32.5V^{-1} for GaAs devices and an improvement to 33V^{-1} from 12.6V^{-1} for $In_{0.53}Ga_{0.47}As$ device. These improvement has been achieved through the insertion 6nm well layer for both QW-$In_{0.18}Ga_{0.82}As$ and QW-$In_{0.8}Ga_{0.2}As$ that consistent to the barrier(AlAs) of 10MLs thickness for standard GaAs/InGaAs respectively. RF simulations were performed for ASPAT devices. It is exhibit that the presence of the Quantum well reduce the C_j at zero voltage bias. C_j was reduced from 34fF and 22.2fF for both conventional diodes to 17.2fF and 10.5fF for proposed structure diodes, respectively. Based on this conclude, the cut off frequencies of the novel 16μm^2 QW ASPATs proposed in this work are increased and expected to be around 143GHz and 303GHz for both structures respectively. Therefore, the proposed QW-ASPAT diodes can be used as an insensitive-temperature detector in the high frequency applications.

Acknowledgements

This research project is supported by University of Mosul, College of Engineering, Mosul, Iraq.

Authors: Shamil H. Hussein, and Prof. Dr. Khalid K. Mohammed, Department of Electrical Engineering, University of Mosul, Mosul, 41002, Iraq, E-mail:shamil_alnajjar84@uomosul.edu.iq,

REFERENCES

[1] N. Oshima, K. Hashimoto, S. Suzuki, and M. Asada, "Wireless data transmission of 34 Gbit/s at a 500-GHz range using resonant-tunnelling-diode terahertz oscillator," *Electronics letters*, vol. 52, no. 22, pp. 1897–1898, 2016.

[2] M. Missous, M. J. Kelly, and J. Sexton, "Extremely uniform tunnel barriers for low-cost device manufacture," *IEEE Electron Device Letters*, vol. 36, no. 6, pp. 543–545, 2015.

[3] A. Salhi, J. Sexton, S. Muttlak, O. Abdulwahid, A. Hadfield, and M. Missous, "InGaAs/AlAs/GaAs metamorphic asymmetric spacer layer tunnel (mASPAT) diodes for microwaves and millimeter-waves detection," *Journal of Applied Physics*, vol. 127, no. 19, p. 194505, 2020.

[4] N. Tuomisto, A. Zugarramurdi, and M. J. Puska, "Modeling of electron tunneling through a tilted potential barrier," *Journal of Applied Physics*, vol. 121, no. 13, p. 134304, 2017.

[5] M. Akura, G. Dunn, and M. Missous, "A hybrid planar-doped potential-well barrier diode for detector applications," *IEEE Transactions on Electron Devices*, vol. 64, no. 10, pp. 4031–4035, 2017.

[6] M. R. Abdullah, Y. Wang, J. Sexton, M. Missous, and M. Kelly, "GaAs/AlAs tunnelling structure: Temperature dependence of ASPAT detectors," 2015, pp. 1–4.

[7] Y. Wang, M. R. R. Abdullah, J. Sexton, and M. Missous, "Temperature dependence characteristics of In0. 53Ga0. 47As/AlAs asymmetric spacer-layer tunnel (ASPAT) diode detectors," 2015, pp. 1–4.

[8] A. Hadfield, A. Salhi, J. Sexton, and M. Missous, "Experimentally Validated Physical Modelling of Asymmetric Spacer Layer Tunnel Diodes for THz Applications," 2019, pp. 1–3.

[9] R. T. Syme, M. J. Kelly, M. Robinson, R. Smith, and I. Dale, "Novel GaAs/AlAs tunnel structures as microwave detectors," 1992, vol. 1675, pp. 46–56.

[10] K. Z. Ariffin *et al.*, "Asymmetric spacer layer tunnel diode (ASPAT), quantum structure design linked to current-voltage characteristics: A physical simulation study," 2017, pp. 1–4.

[11] A. J. Hadfield, "Heterostructure Tunnel Diodes for Terahertz and mm-Wave applications," 2021.

[12] A. S. Hajo, O. Yilmazoglu, F. Küppers, and T. Kusserow, "Integration and characterisation of Schottky diodes with a pre-amplifier for THz applications," 2020, pp. 1–2.

[13] J. Karlovský, "The curvature coefficient of germanium tunnel and backward diodes," *solid-state Electronics*, vol. 10, no. 11, pp. 1109–1111, 1967.

[14] O. Abdulwahid, S. G. Muttlak, J. Sexton, M. Missous, and M. Kelly, "24ghz zero-bias asymmetrical spacer layer tunnel diode detectors," 2019, pp. 1–3.

[15] A. Hadfield, A. Salhi, J. Sexton, and M. Missous, "Novel barrier-well heterostructure diodes for microwave and mm-wave applications," *Solid-State Electronics*, vol. 178, p. 107963, 2021.

[16] A. Salhi, A. Hadfield, S. Muttlak, J. Sexton, M. Kelly, and M. Missous, "Design and analysis of GaAs/AlAs asymmetric spacer layer tunnel diodes for high-frequency detection," *Physica E: Low-dimensional Systems and Nanostructures*, vol. 130, p. 114723, 2021.

[17] S. H. Hussein and K. K. Mohammed, "A miniaturized advanced rectenna integrated circuit for implantable applications," AEU-International Journal of Electronics and Communications, p. 154544, 2023..